Synthesis of Bioorganometallic Nanomolar Potent CB_2 Agonists Containing a Ferrocene Unit.

Supojjanee Sansook[#,°], Wei Tuo[⊥,°], Lucas Lemaire[⊥], Aurélien Tourteau[⊥], Amélie Barczyk[⊥], Xavier Dezitter[⊥], Frédérique Klupsch[⊥], Natascha Leleu-Chavain[⊥], Graham J. Tizzard[≠], Simon J. Coles[≠], Rėgis Millet[⊥,*] John Spencer[#,*]

Abstract. A small library of ferrocene containing amides have been synthesized using standard amide coupling chemistry with ferrocenylamine. Ferrocene analogues of known bioactive adamantylamides were shown to be effective cannabinoid receptor (CB_1 and CB_2) agonists, displaying, in many cases, single digit nM potency. Three final ferrocene-containing derivatives have been characterized in the solid state by X-ray crystallography and display intramolecular hydrogen bonding of the type NH---C=O. N-Methylation of the amide, confirmed by X-ray crystallography, leads to loss of hydrogen bonding and biological activity.

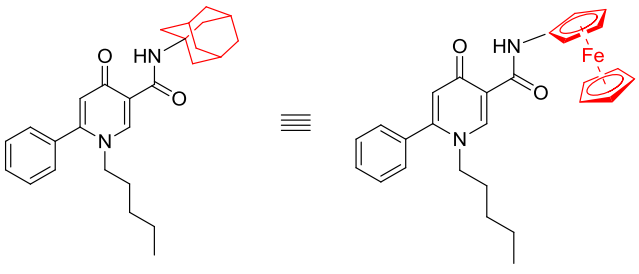

K_i CB_2 =4 nM
E_{max} cAMP = 458%
EC_{50} cAMP = 12 nM

K_i CB_2 =5 nM
E_{max} cAMP = 500%
EC_{50} cAMP = 12 nM

[#]Department of Chemistry, School of Life Sciences, University of Sussex, Falmer, Brighton, East Sussex, BN1 9QJ, UK. [≠]UK National Crystallography Service, School of Chemistry, University of Southampton, Highfield, Southampton, SO17 1BJ, UK. [⊥]ICPAL, Univ. Lille,

Inserm, U995-LIRIC-Lille Inflammation Research International Center, 3 rue du Professeur Laguesse, BP83, F-59006 Lille, France.

Corresponding authors: j.spencer@sussex.ac.uk; regis.millet@univ-lille2.fr.

° Both authors contributed equally to the manuscript.

Keywords: bioorganometallic; GPCR; aminoferrocene.

Introduction. Cannabinoid receptors, belonging to the G-protein-coupled receptors (GPCR) superfamily, consist of two subtypes CB_1 and CB_2. The latter are widely distributed in the immune system, whereas CB_1 receptors are predominately located in the central nervous system.[1-3] According to their high distribution in the immune system, CB_2 receptors have been suggested to play a crucial role in the modulation of inflammation.[4] Overexpression of CB_2 receptors is observed after an inflammation stimuli.[5] Activation of CB_2 receptors is accompanied by the suppression of macrophages activation, the blockage of calcium signals in nociceptors and the modulation of nociceptor excitability, associated with anti-inflammation, anti-nociception, neuroprotection, gastroprotection or other protective effects.[6, 7] Moreover, activation of CB_2 receptors rather than CB_1 receptors has been identified to be devoid of cannabimimetic side effects (such as hypomotility, hypothermia and catalepsy).[8]

At the molecular level, the CB_2 receptor is coupled to a $G\alpha_{i/0}$ subunit that inhibits adenylyl cyclase and cyclic adenosine monophosphate (cAMP) production. According to their functionality, ligands for CB_2 receptors can be classified as : (1) agonists, which activate CB_2 receptors and then repress adenylyl cyclase, thereby resulting in a decrease in cAMP concentration, (2) antagonists, which prevent the activation of receptors by endocannabinoids, and (3) inverse agonists, which reduce CB_2 receptor activity and induce an accumulation of cAMP through upregulation of adenylyl cyclase activity.[9, 10] CB_2 agonists have been demonstrated to produce anti-inflammatory, analgesic, and other protective efficacies by the modulation of calcium signal and nociceptor excitability.[6, 11] CB_2 antagonists/inverse agonists have been argued to show potential in the treatment of bone-dependent disorders (such as osteoporosis) through regulation of bone proliferation.[12-15] In addition, inverse agonists have been identified to exert immunomodulatory ability and therapeutic potential for inflammation (such as carrageenan-induced paw swelling) through regulating the migration of inflammatory cells and immune cells, including leukocytes.[12, 13, 16]

Accordingly, the development of CB_2 ligands has been viewed as an interesting approach for the treatment of a wide range of nervous or immune system disorders. Over the last decades, research on CB_2 ligands has significantly progressed. Several CB_2 agonists, antagonists, and inverse agonists have been disclosed. (*R*)-(+)-[2,3-Dihydro-5-methyl-3-(4-morpholinylmethyl)pyrrolo[1,2,3-de]-1,4-benzoxazin-6-yl]-1-napthalenylmethanone **1** (WIN 55,212-2, Figure 1), one of the most potent dual CB_1/CB_2 agonists to date, has been widely used for the investigation of cannabinoid receptor-dependent biological responses.[17] It exerts antinociceptive efficacy in a model of neuropathic spinal cord injury and inhibits the proliferation of cancer cells.[18, 19] (2-Iodo-5-nitrophenyl)-[1-[(1-methylpiperidin-2-yl)methyl]indol-3-yl]methanone **2** (AM-1241, Figure 1), an aminoalkylindole derivative, has been demonstrated to be a potent selective CB_2 agonist and shows efficacy in a variety of *in vivo* pain and inflammation models, including spinal nerve ligation (SNL)-induced nociception and 2,4,6-trinitrobenzenesulfonic acid (TNBS)-induced colitis.[20, 21] Compound **3** (SR144528, Figure 1) was the first selective CB_2 antagonist, discovered by Sanofi Research, and was later identified to possess temperature-dependent inverse agonist properties.[22-24] It was further identified to up-regulate the expression of CB_2 receptors.[23, 25] 6-Iodopravadoline **4** (AM630, Figure 1), a potent selective CB_2 inverse agonist, showed potential to attenuate titanium particle-induced osteoporosis.[26, 27] Two other well-known CB_2 inverse agonists **5** (Sch225336, Figure 1) and **6** (Sch414319, Figure 1) manifest the ability to relieve inflammation by modulating the migration of immune cells.[12, 16]

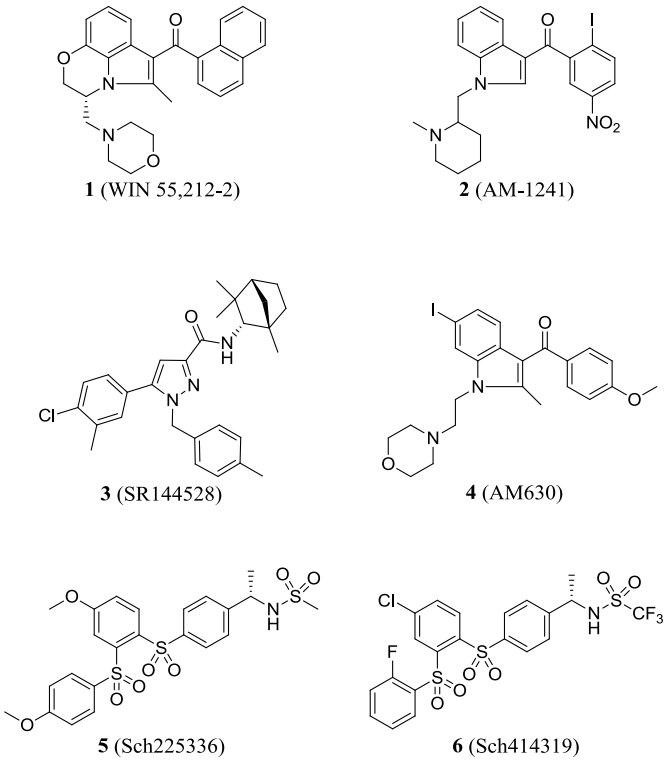

Figure 1. Structures of representative CB_2 ligands.

Previously, 4-oxo-1,4-dihydropyridine and 4-oxo-1,4-dihydroquinoline have been demonstrated to be favorable scaffolds for the design of potent CB_2 agonists or inverse agonists.[28-31] Specifically, derivatives bearing a 1-adamantylamine group were determined to be potent and functionally-selective CB_2 ligands. For instance, the 4-oxo-1,4-dihydroquinoline derivative **7** (Figure 2) was identified as a CB_2 agonist (K_i = 16.4 nM, E_{max} (GTPγS) = 125.6%). In the 4-oxo-1,4-dihydropyridines series, derivative **8** (Figure 2) showed partial agonist properties, while compound **9** (Figure 2) was identified as a full agonist for CB_2 receptors (K_i = 20 and 29 nM, E_{max} (GTPγS) = 148% and 212%, EC_{50} (GTPγS) = 5.5 nM and 12.2 nM, respectively).[32] These compounds showed good selectivity over CB_1 receptors (Selectivity index (SI) > 100).[30] Conversely, another 4-oxo-1,4-dihydropyridine derivative **10** (K_i = 4 nM, E_{max} (GTPγS) = 39%, EC_{50} (GTPγS) = 3.2 nM, SI = 148, Figure 2) bearing a phenyl ring instead of an alkyl group at C6 position behaves as a CB_2 inverse agonist.[30]

Depending on the substituent at position-6 (methyl, tert-butyl or phenyl group), the biological response changes from CB_2 agonist to CB_2 inverse agonist. This switch is supposedly due to interactions between the 6-substituted phenyl ring and Trp258 of the receptor. It has been demonstrated that the phenyl ring at the C6 position of 4-oxo-1,4-dihydropyridines confers inverse agonist properties through the stabilization of χ_1 torsion of the Trp258 side chain in its inactive conformation,[30] thereby inducing a CB_2-mediated inverse biological response associated with the upregulated production of cAMP.

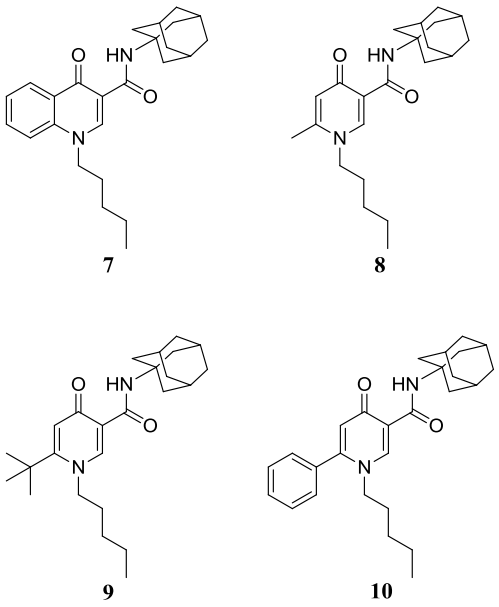

Figure 2. Structures of previously developed 4-oxo-1,4-dihydropyridine/4-oxo-1,4-dihydroquinoline-derived CB_2 ligands containing an adamantylamine group.

Ferrocene, an organometallic complex, shows advantageous properties for the design of potential pharmaceutical agents. For instance, its lipophilicity (logP = 2.66 (ferrocene) *vs.* 2.69 for adamantane) endows its derivatives with suitable bioavailability and membrane penetration.[33-35] The rotation of the aromatic cyclopentadienyl ring confers conformation diversity on ferrocene (staggered or overlapped conformation), which is favorable for orientating ferrocene-derived ligands into their receptor pockets.[36] Additionally, ferrocene derivatives have been identified to produce a variety of biological responses, including anticancer,[36-47] antimalarial,[36, 48] antioxidant,[49] antibacterial[50] and glucose sensing

properties.[51] Thus, development of ferrocene derivatives could be regarded as an interesting approach to discover potential novel pharmaceutical agents and tool compounds.

Based on these interesting results, we decided to observe the influence of the replacement of the 1-adamantyl group by a ferrocene unit. Herein, we report the synthesis and biological evaluation of a novel series of ferrocenyl 4-oxo-1,4-dihydropyridine and dihydroquinoline derivatives. Both series of compounds were easily synthesized by standard amide coupling protocols and were characterized by ^{1}H and ^{13}C NMR spectroscopy, mass spectrometry and combustion analysis, for solids, or by percentage purity by LCMS for oils (Scheme 1). In the case of solids, four of these air-stable derivatives were further characterized in the solid state by X-ray crystallography, confirming the presence of intramolecular hydrogen bond between the ketone and amide functionalities, which is also observed in solution-based studies (δ=ca. 11.5 ppm in their ^{1}H NMR spectra). Compound **11b** exhibits some minor disorder in the solid state with the substituent pentyl chain adopting two slightly different conformations in the approximate ratio 57:43.

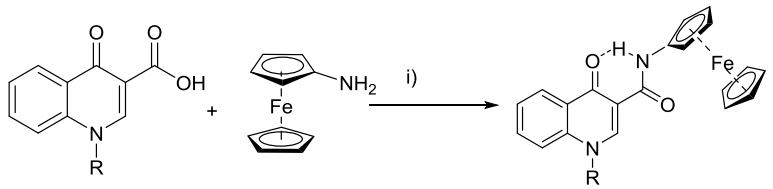

11a: R=Cy, 75%.
11b: R=n-Pent, 43%.
11c; R=CH_2CH_2-N-morphinyl, 47%.

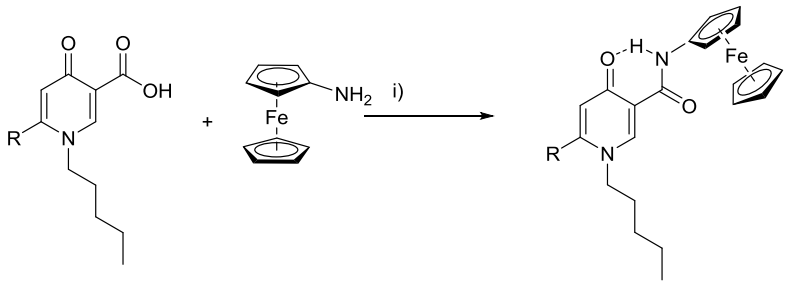

12a; R=CH_3, 52%.
12b, R=t-Bu, 49%.
12c; R=Ph, 62%.

i) HOBt, HBTU, DIEPA, $CHCl_3$, RT 24 h.

Scheme 1. Synthesis of ferrocenylamides.

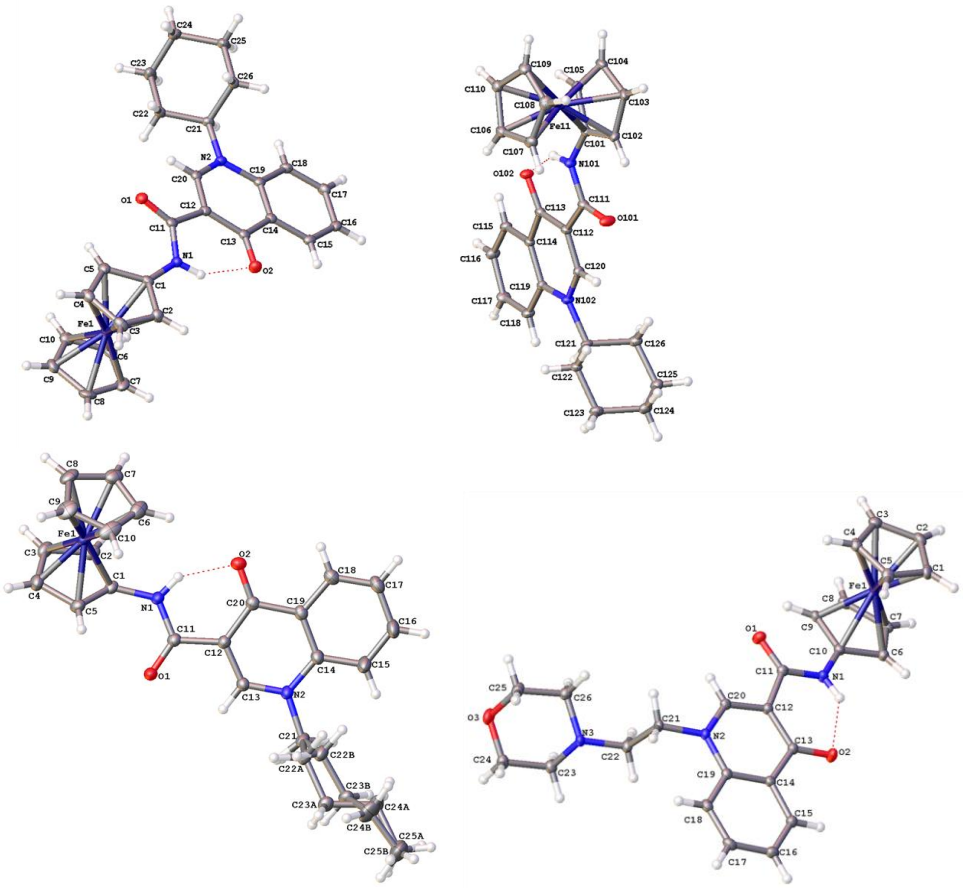

Figure 3. Solid state structures of ferrocene products: **11a** (top), **11b** (bottom left), and **11c** (bottom right).

Often, an intramolecular hydrogen bond acts as a conformational lock, stabilizing an active conformation of a molecule and improving its binding to a receptor or enzyme.[52] Given that all the ferrocenes synthesized herein display such hydrogen bonding (Figure 3) we decided to synthesize a *N*-Me amide derivative **13a** to compare its receptor binding to its NH-amide precursor **11a** (Scheme 2). The ^{1}H NMR spectrum of **13a**, even at variable temperature (VT), showed a broad signal and was indicative of a fluxional molecule. Nevertheless, we confirmed its structure by X-ray crystallography (Scheme 2), which clearly shows a change in conformation brought about by the loss of the intramolecular H-bond.

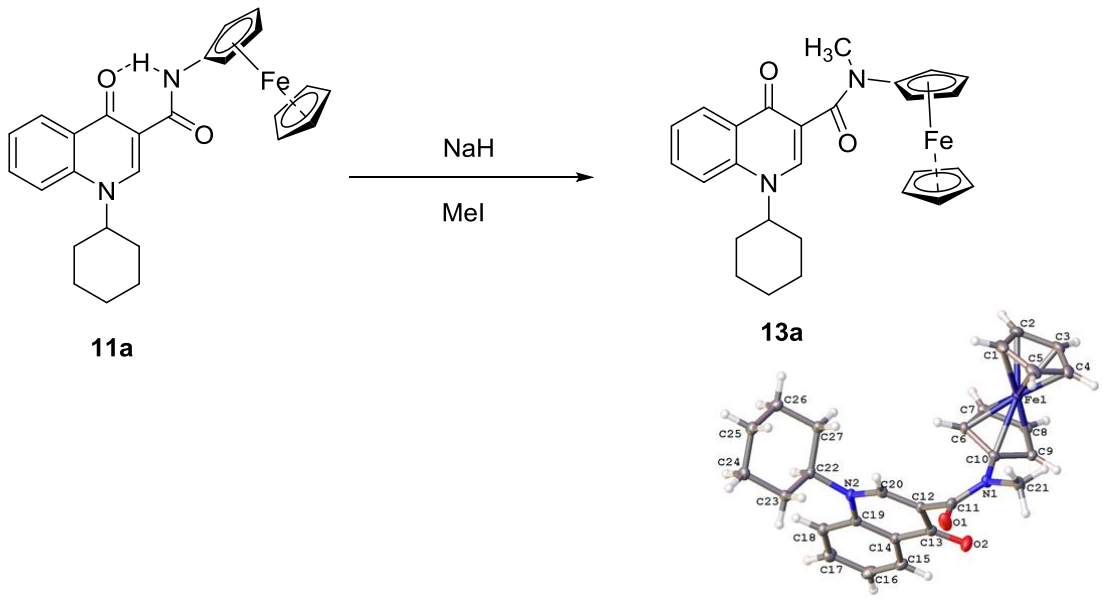

Scheme 2. *N*-Methylation reaction of a ferrocenyl amide.

The affinities of each synthesized compound for both CB_1 and CB_2 receptors were determined by a competitive radioligand displacement assay using the dual CB_1/CB_2 ligand [^{3}H]-CP55,940.[53, 54]

Compounds **11a**, **11b**, **11c**, **12a**, **12b**, and **12c** manifest good CB_2 affinity (5 nM < K_i < 220 nM). Specifically, for the 4-oxo-1,4-dihydroquinoline derivatives, a lipophilic alkyl chain on the endocyclic nitrogen (**11a**, K_i = 36.7 nM; **11b**, K_i = 10.9 nM) gives a superior affinity to the compound than a hydrophilic morpholinoethyl group (**11c**, K_i = 133.6 nM). As expected, the methylation of the amide group of compound **11a** brought about a sharp decrease in affinity for CB_2 (**13a**, K_i > 1 μM). In the 4-oxo-1,4-dihydropyridine series , a bulky group (such as a *tert*-butyl or a phenyl group, **12b**, K_i = 59.5 nM and **12c**, K_i = 5.2 nM, respectively) is preferred for CB_2 affinity rather than a small alkyl group (such as a methyl, **12a**, K_i = 218.8 nM) at the C6 position. Compared to previously developed CB_2 ligands (such as **7**, **8**, **9** and **10**, SI > 100), the replacement of the 1-adamantyl group by a ferrocene seems to maintain the CB_2 affinity of the molecules, with only a weak decrease in affinity for **12a** compared to **8**.

However, it brings about an obvious increase in affinity for CB_1 receptors (**12a**, **12b**, and **12c**, SI < 15).

Compounds displaying potent CB_2 affinity were further studied for their functionality by cAMP assays in Chinese hamster ovary cells expressing CB_2 receptors (CHO-CB_2).[55-57] Cells were treated with forskolin in order to activate adenylyl cyclase and cAMP production. In Table 1, the maximum efficacy (E_{max}) of a compound represents the maximum response at 10^{-6} M and is expressed as the percentage of forskolin-induced cAMP production. Compound potency was also evaluated in the presence of increasing concentrations of each compound and was expressed as the concentration that exhibits the half-maximal response (EC_{50}). Although 4-oxo-1,4-dihydroquinolines **11a** and **11b** were determined to show potent affinity for CB_2 receptors, their binding to the receptors did not significantly affect CB_2-mediated regulation of cAMP production (E_{max} cAMP = 74% and 78%, respectively). The replacement of the *N*-substituted alkyl group of 4-oxo-1,4-dihydroquinoline-3-carboxamide derivatives by an *N*-ethyl morpholine gave rise to an obvious increase in CB_2 agonist functionality of the molecule (**11c**, E_{max} cAMP = 52%), which might be attributed to probable hydrogen binding interactions between morpholine and CB_2 receptors. The 4-oxo-1,4-dihydropyridine-3-carboxamide derivatives bearing an alkyl substituent at C6 position (**12a** and **12b**) show CB_2 agonist properties (E_{max} cAMP = 50% and 55%, respectively). In the 4-oxo-1,4-dihydropyridine-3-carboxamide series, compound **12c** (E_{max} cAMP = 500%), bearing a 6-substituted phenyl group instead of an alkyl substituent, appears to behave as a CB_2 inverse agonist. These observations are consistent with our previous results.[4] It is noteworthy that **12c**-induced accumulation of cAMP (EC_{50} cAMP = 12 nM) is approximately 65-fold more greater than for compound **4** (EC_{50} cAMP = 785 nM), one of the most potent CB_2 inverse agonists reported to date. Interestingly, as illustrated in Table 1, replacement of the 1-

adamantyl group (**8**, **9**, and **10**) by a ferrocene (**12a**, **12b**, and **12c**) does not alter the functionality of these compounds and their ability to regulate cAMP formation.

The cytotoxicity of these compounds was determined at 10 μM using a cell proliferation assay on Chinese hamster ovary cells wild type (CHO-WT), CHO-CB_2 and human colorectal adenocarcinoma cells HT29. This test is based on a colorimetric method, which measures the activity of cellular enzymes that reduce the tetrazolium dye (MTS, yellow) to its insoluble formazan giving a purple color. This assay measures cellular metabolic activity *via* NADPH-dependent cellular oxidoreductase enzymes and reflects, under defined conditions, the number of viable cells. No significant cytotoxicity was observed for these new compounds except for derivative **11c**, which slightly inhibited the proliferation of HT29 cells (48% at 10 μM).[58]

Table 1. Affinities (K_i values), maximum efficacy (E_{max}), and/or half-maximal response (EC_{50}) of compounds **8-10**, **11a-c**, **12a-c**, **13a** and reference compounds (WIN-55,212-2, AM630) towards *h*CB_2 and *h*CB_1 cannabinoid receptors, selectivity ratios *h*CB_2 *versus* *h*CB_1, and cytotoxicity on CHO-WT, CHO-CB_2, and HT29 cells

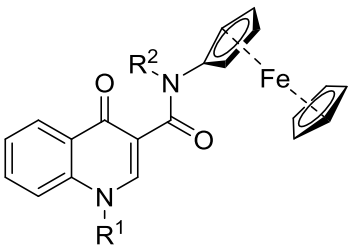

11a-c, **13a**

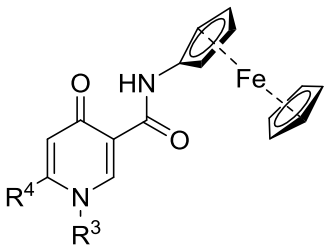

12a-12c

Compounds	Substituents		*h*CB_2 and *h*CB_1 binding assays[a]			CB_2 cAMP assay[a]		Cytotoxicity assays % inhibition at 10 μM		
	R^1	R^2	CB_2 K_i (nM)	CB_1 K_i (nM)	Ratio CB_1/CB_2	E_{max} (%)[b]	EC_{50} (nM)	CHO-WT	CHO-CB_2	HT29
8			20 ± 3[c]	> 3000[c]	> 150[c]	63 ± 8	8.0 ± 3.3	N. D.[d]	N. D.[d]	N. D.[d]
9			29 ± 3[c]	> 3000[c]	> 103[c]	51 ± 14	21 ± 10	N. D.[d]	N. D.[d]	N. D.[d]
10			4.0 ± 0.4[c]	592 ± 97[c]	148[c]	458 ± 106	36 ± 6	N. D.[d]	N. D.[d]	N. D.[d]
11a	Cyclohexyl	H	36.7 ± 20.4	372.2 ± 27.6	10.1	74 ± 13	N. D.[d]	0	0	0
11b	*n*-Pentyl	H	10.9 ± 2.2	5.5 ± 2.0	0.5	78 ± 14	N. D.[d]	0	0	0
11c	Morpholinoethyl	H	133.6 ± 25.6	475.4 ± 51.7	3.6	52 ± 9	9.9 ± 1.5	0	5	48
13a	Cyclohexyl	Methyl	> 1000	N. D.[d]	N. D.[d]	N. D.[d]	N. D.[d]	0	0	0
	R^3	R^4								
12a	*n*-Pentyl	Methyl	218.8 ± 15.8	204.9 ± 33.7	0.9	50 ± 14	11.0 ± 4.9	0	0	1
12b	*n*-Pentyl	*t*-Butyl	59.5 ± 13.8	747.2 ± 106.1	12.6	55 ± 13	21 ± 14	0	0	0
12c	*n*-Pentyl	Phenyl	5.2 ± 0.4	23.4 ± 1.9	4.5	500 ± 32	12.0 ± 1.5	0	0	0
Forskolin						100				
WIN55,212-2			6.9 ± 2.0	13.9 ± 4.0	2.0	45 ± 7	4.3 ± 1.1			
AM630			31.2 ± 12.4[e]	5152 ± 567[e]	165[e]	232 ± 79	785 ± 7			

[a] Data represent the mean ± SEM of three or four experiments performed in duplicate or triplicate.
[b] E_{max} values are expressed as a percentage of forskolin-induced cAMP production.
[c] Data from Ref 30.
[d] N. D. means not determined.
[e] Data from Ref 26.

Conclusions. A small library of ferrocenylamine-based 4-oxo-1,4-dihydropyridine and dihydroquinoline derivatives has been synthesized. Many display potency even at low (nM) concentrations *vs*. CB_1 and CB_2 receptors. A crucial intramolecular (NH---O=C) hydrogen bond, evidenced in both solution and the solid state, appears to be important for receptor binding since N-methylation, and subsequent loss of this hydrogen bond, leads to a loss of affinity. This study demonstrates that aminoferrocene-based compounds can replace adamantanyl amines in GPCR-targeting bioorganometallic agents. Whether or not this effect is simply a size/shape similarity of a ferrocene moiety compared to an adamantly group or if there is the induction of reactive oxygen species (ROS) as is often the case with ferrocenyl groups in bioorganometallic chemistry is beyond the scope of this study but the latter cannot be ruled out.[41, 44, 59-61]

Statement. The authors declare no competing financial interests.

Experimental

Solvents and reagents were purchased from commercial suppliers and were used without purification. Ferrrocenylamine was purchased from TCI, UK and used as such. All reactions were performed in a fume hood. NMR spectra were recorded on Varian 500 MHz or 400 MHz spectrometers and chemical shifts are reported in ppm, usually referenced to TMS as an internal standard. LCMS were performed on a 5 μm C18 110 Å column and percentage purities were ran over 30 minutes in water/acetonitrile with 0.1% formic acid (5 min at 5%, 5%-95% over 20 min, 5 min at 95%) with the UV detector at 254 nm. High resolution mass spectrometry (HRMS) were performed by the EPSRC National Mass Spectrometry Facility, University of Swansea. Elemental Analyses were conducted by Stephen Boyer (London Metropolitan University).

1-Cyclohexyl-*N*-ferrocenyl-4-oxo-*N*-ferrocenyl-1,4-dihydroquinoline-3-carboxamide (**11a**). The title compound was prepared by a coupling reaction; 1-cyclohexyl-4-oxo-1,4-dihydroquinoline-3-carboxylic acid (271 mg, 1 mmol) was reacted with HOBt (68 mg, 0.5 mmol) , HBTU (570 mg, 1.5 mmol) and DIPEA (0.35 mL) in $CHCl_3$ solution (20 mL). The reaction mixture was stirred at RT for 45 min. and then aminoferrocene (241 mg, 1.2 mmol) was added and the mixture was stirred for 24 h. Afterwards, the reaction mixture was washed with NaOH (0.5N, 20 mL), HCl (1N, 20 mL) and H_2O (20 mL). The organic layer was dried with $MgSO_4$ and evaporated to 3 mL volume and purified by column chromatography. The

orange band was eluted with a hexane: ethyl acetate (7:3) mixture, and was collected and evaporated to dryness. The yield was 340 mg, 75% (orange solid). Crystallization by diffusion between CH_2Cl_2 and hexane provided orange crystals. ^{1}H NMR ($CDCl_3$) 500 MHz. δ = 11.56 (1H, s, NH), 9.04 (1H, s, CH), 8.62 (1H, dd, $^3J_{HH}$ = 8.1, $^4J_{HH}$ = 1.6, CH), 7.78 – 7.76 (1H, m, CH), 7.68 (1H, d, $^3J_{HH}$ = 8.7, CH), 7.55 - 7.53(1H, m, CH), 4.82 (2H, d, $^3J_{HH}$ = 1.8 , CH_2), 4.53- 4.51 (1H, m, CH), 4.19 (5H, s, Cp), 4.05 (2H, d, $^3J_{HH}$ = 1.8, CH_2), 2.22- 2.19 (2H, m, CH_2), 2.08 – 2.05 (2H, m, CH_2), 1.89 – 1.86 (3H, m, CH_2+CH), 1.60-1.57 (2H, m, CH_2), 1.36 - 1.34 (1H, m, CH). ^{13}C NMR ($CDCl_3$) 126 MHz. δ = 176.2, 163.2, 143.1, 139.4, 132.8, 128.1, 127.6, 125.0, 115.2, 111.8, 94.5, 69.2, 64.5, 61.8, 59.8, 32.8, 25.9, 25.2. HRMS-ESI (m/z) found 455.1396, calcd for $[C_{26}H_{26}FeN_2O_2 + H]^+$ 455.1416. Elemental Analysis: calcd (%) C, 68.73; H, 5.77; N, 6.17 for $C_{26}H_{26}FeN_2O_2$; fnd (%) C, 68.50; H, 5.89; N, 6.06.

***N*-Ferrocenyl-4-oxo-1-pentyl-1,4-dihydroquinoline-3-carboxamide** (**11b**). 4-Oxo-1-pentyl-1,4-dihydroquinoline-3-carboxylic acid (25.9 mg, 0.1 mmol) was reacted with HOBt (6.8 mg, 0.05 mmol), HBTU (57 mg, 0.15 mmol) and DIPEA (0.035 mL) in $CHCl_3$ solution (2 mL). The reaction mixture was stirred at RT for 45 min. and then aminoferrocene (24.1 mg, 0.12 mmol) was added and the mixture was stirred for 24 h. Work-up was as above. The orange band was eluted with a hexane: ethyl acetate (1:1) mixture, and was collected and evaporated to dryness. The yield was 19 mg, 43% (orange solid). Crystallization by diffusion between CH_2Cl_2 and hexane provided yellow crystals. ^{1}H NMR ($CDCl_3$) 500MHz. δ = 11.51 (1H, s, NH), 8.84 (1H, s, CH), 8.61 - 8.58 (1H, m, CH), 7.79 – 7.77 (1H, m, CH), 7.54 - 7.52 (2H, m, Ar), 4.81 (2H, d, $^3J_{HH}$ = 1.9, CH_2), 4.30 – 4.27 (2H, m, CH_2), 4.20 (5H, s, Cp), 4.05 (2H, d, $^3J_{HH}$ = 1.9, Cp), 1.42 - 1.38 (6H, m, 3CH_2), 0.94 - 0.90 (3H, m, CH_3). ^{13}C ($CDCl_3$) 126 MHz. δ = 176.6, 163.1, 147.4, 139.0, 132.9, 128.0, 127.5, 125.2, 115.9, 111.9, 94.4, 69.2, 64.6, 62.0, 54.4, 28.7, 28.8, 22.2, 13.8. HRMS-ESI (m/z) found 443.1412, calc. for $[C_{25}H_{26}FeN_2O_2 + H]^+$ 443.1416. Elemental Analysis: calcd (%) C, 67.88; H, 5.92; N, 6.33 for $C_{25}H_{26}FeN_2O_2$: Fnd (%) C, 67.87; H, 6.05; N, 6.45.

***N*-Ferrocenyl-1-(2-morpholinoethyl)-4-oxo-1,4-dihydroquinoline-3-carboxamide** (**11c**). 1-(2-Morpholinoethyl)-4-oxo-1,4-dihydroquinoline-3-carboxylic acid (30.2 mg, 0.1 mmol) was reacted with HOBt (6.8 mg, 0.05 mmol) , HBTU (57 mg, 0.15 mmol) and DIPEA (0.035 mL) in $CHCl_3$ solution (2 mL). The reaction mixture was stirred at RT for 45 min. and then aminoferrocene (24.1 mg, 0.12 mmol) was added and the mixture was stirred for 24 h. Work-up was as above. The orange band was eluted with a hexane: ethyl acetate (3:7) mixture, and

was collected and evaporated to dryness. The yield was 23 mg, 47% (yellow solid). Crystallization by diffusion between acetone and hexane provided orange crystals. ^{1}H NMR ($CDCl_3$) 500 MHz. δ = 11.46 (1H, s, NH), 8.84 (1H, s, CH), 8.60 (1H, dd, $^{3}J_{HH}$ = 8.1, $^{4}J_{HH}$ = 1.5, CH), 7.79 – 7.76 (1H, m, CH), 7.58 - 7.54 (2H, m, Ar), 4.82- 4.79 (1H, m, CH), 4.39 (2H, d, $^{3}J_{HH}$ = 1.9, CH_2), 4.20 (5H, s), 4.13 – 4.11 (1H, m, CH), 4.08 – 4.05 (1H, m, CH), 3.70 – 3.68 (2H, m, CH_2), 2.85 – 2.83 (1H, m, CH), 2.53 (2H, m, CH_2), 2.05 (1H, s, CH), 1.29 -1.26 (3H, m). ^{13}C ($CDCl_3$) 126 MHz. δ = 176.6, 162.9, 148.2, 139.0, 133.0, 128.0, 127.6, 125.2, 115.6, 111.8, 94.3, 69.2, 66.8, 64.6, 62.0, 56.5, 53.8, 51.4. HRMS-ESI (m/z) found 486.1471, calcd. for $[C_{26}H_{27}FeN_3O_3 + H]^+$ 486.1475. Elemental Analysis. Calcd (%) C, 64.34; H, 5.61; N, 8.66 for $C_{26}H_{27}FeN_3O_3$: Fnd (%) C, 64.27; H, 5.54; N, 8.63.

***N*-Ferrocenyl-6-methyl-4-oxo-1-pentyl-1,4-dihydropyridine-3-carboxamide** (**12a**). 6-Methyl-4-oxo-1-pentyl-1,4-dihydropyridine-3-carboxylic acid (22.3 mg, 0.1 mmol) was combined with HOBt (6.8 mg, 0.05 mmol) , HBTU (57 mg, 0.15 mmol) and DIPEA (0.035 mL) in $CHCl_3$ (2 mL). The reaction mixture was stirred at RT for 45 min and then aminoferrocene (24.1 mg, 0.12 mmol) was added. Work-up was as above. The orange band was eluted with a hexane: ethyl acetate (2:3) mixture, and was collected and evaporated to dryness. The yield was 21 mg, 52% (orange oil). ^{1}H NMR ($CDCl_3$) 500MHz. δ = 11.72 (1H, s, NH), 8.45 (1H, s, CH), 6.46 (1H, s, CH), 4.88- 4.84 (2H, m, CH_2), 4.24 (5H, s, Cp), 4.15 – 4.12 (2H, m, CH_2), 3.91 (2H, d, $^{3}J_{HH}$ = 1.9, Cp), 2.39 (3H, s, CH_3), 1.80- 1.76 (2H, m, CH_2), 1.38 – 1.32 (4H, m, $2CH_2$), 0.94 – 0.90 (3H, m, CH_3). ^{13}C ($CDCl_3$) 126 MHz. δ = 177.4, 162.4, 147.8, 144.9, 121.4, 118.9, 69.6, 65.0, 62.0, 53.9, 30.6, 29.7, 28.5, 22.2, 19.0, 13.8. HRMS-ESI(m/z) found 407.1414 , calc. for $[C_{22}H_{26}FeN_2O_2 + H]^+$ 407.1416. LCMS purity (UV) = 100%, Ret. Time 19.13 min. LCMS purity (Positive ion, TIC) = 93.5%, Ret. Time 19.20 min.

6-tert-Butyl-*N*-ferrocenyl-4-oxo-1-pentyl-1,4-dihydropyridine-3-carboxamide (**12b**). 6-(*tert*-Butyl)-4-oxo-1-pentyl-1,4-dihydropyridine-3-carboxylic acid (26.5 mg, 0.1 mmol) was combined with HOBt (6.8 mg, 0.05 mmol) , HBTU (57 mg, 0.15 mmol) and DIPEA (0.035 mL) in $CHCl_3$ (2 mL). The reaction mixture was stirred at RT for 45 min. and then aminoferrocene (24.1 mg, 0.12 mmol) was added and the mixture was stirred for 24 h. Work-up was as above. The orange band was eluted with a hexane: ethyl acetate (1:1) mixture, which was collected and evaporated to dryness. The yield was 22 mg, 49% (orange oil). ^{1}H NMR ($CDCl_3$) 500 MHz. δ = 11.70 (1H, s, NH), 8.48 (1H, s, CH), 6.66 (1H, s, CH), 4.78 – 4.76 (2H, m, CH_2), 4.16 (5H, s, Cp), 4.13 – 4.10 (2H, m, CH_2) 4.04 - 4.02 (2H, m, CH_2), 2.19

– 2.15 (2H, m, CH_2), 1.46 (9H, s, t-Bu), 1.42 – 1.38 (4H, m, $2CH_2$), 0.98 - 0.92 (3H, m, CH_3). ^{13}C ($CDCl_3$) 126 MHz. 177.7, 162.4, 158.5, 147.0, 119.0, 118.2, 110.0, 94.0, 69.2, 64.6, 62.1, 59.5, 54.9, 35.8, 32.0, 30.4, 28.7, 22.2, 13.9. HRMS-ESI(m/z) found 449.1886, calc. for $[C_{25}H_{32}FeN_2O_2 + H]^+$ 449.1886. LCMS purity (UV) = 100%, Ret. Time 23.68 min. LCMS purity (Positive ion, TIC) = 96.8%, Ret. Time 23.76 min.

***N*-Ferrocenyl-4-oxo-1-pentyl-6-phenyl-1,4-dihydropyridine-3-carboxamide** (**12c**). 4-Oxo-1-pentyl-6-phenyl-1,4-dihydropyridine-3-carboxylic acid (28.5 mg, 0.1 mmol) was reacted with HOBt (6.8 mg, 0.05 mmol) , HBTU (57 mg, 0.15 mmol) and DIPEA (0.035 mL) in $CHCl_3$ (2 mL). The reaction mixture was stirred at RT for 45 min. and then aminoferrocene (24.1 mg, 0.12 mmol) was added and the mixture stirred for 24 h. Work-up was as above. The orange band was eluted with a hexane: ethyl acetate (1:1) mixture, which was collected and evaporated to dryness. The yield was 29 mg, 62% (orange solid). ^1H NMR ($CDCl_3$) 500 MHz. δ = 11.80 (1H, s, NH), 8.61 (1H, s, CH), 7.56- 7.52 (3H, m, Ar), 7.39 – 7.35 (2H, m, Ar), 6.54 (1H, s, CH), 4.80 (2H, d, $^3J_{HH}$ = 1.9, CH_2), 4.20 (5H, s, Cp), 4.05 (2H, d, $^3J_{HH}$ = 1.9, CH_2), 3.85 – 3.83 (2H, m, CH_2), 1.65 – 1.61 (2H, m, CH_2), 1.18 – 1.16 (4H, m, 2 CH_2), 0.81 (3H, t, $^3J_{HH}$ = 7.1, CH_3). ^{13}C ($CDCl_3$) 126 MHz. δ = 177.1, 162.4, 151.8, 144.8, 133.2, 130.1, 129.0, 128.5, 122.4, 119.4, 93.9, 69.2, 64.7, 62.1, 54.4, 30.6, 28.2, 21.9, 13.7. HRMS-ESI(m/z) found 469.1576 , calc. for $[C_{27}H_{28}FeN_2O_2 + H]^+$ 469.1573. Elemental Analysis: calcd (%) C, 69.24; H, 6.03; N, 5.98 for $C_{27}H_{28}FeN_2O_2$: Fnd (%) C, 68.89; H, 6.13; N, 5.81.

1-Cyclohexyl-*N*-ferrocenyl-*N*-methyl-4-oxo-1,4-dihydroquinoline-3- carboxamide (**13a**). The title compound was prepared by reacting **11a** (110 mg, 0.2 mmol) with NaH (10 mg, 0.4 mmol) in dry DMF(5 mL). The reaction mixture was stirred at RT for 20 min and then iodomethane (45 µL, 0.7 mmol) was added. After stirring at RT overnight the mixture was extracted with EtOAc, then washed with brine, H_2O dried over $MgSO_4$ and evaporated. A yellow band was eluted, using chromatography, with a hexane: ethyl acetate (2:3) mixture, collected and evaporated to dryness. The yield was 38 mg, 41% (yellow solid). Crystallization by diffusion between CH_2Cl_2 and hexane provided yellow crystals. HRMS-ESI(m/z) found 469.1576 , calcd. for $[C_{27}H_{28}FeN_2O_2 + H]^+$ 469.1573. Elemental Analysis; calcd (%) C, 69.24; H, 6.03; N, 5.98 for $C_{27}H_{28}FeN_2O_2$: Fnd (%) C, 69.19; H, 6.10; N, 6.03. LCMS purity (UV) = 100%, Ret. Time 18.20 min. LCMS purity (Positive ion, TIC) = 91.6%, Ret. Time 18.27 min.

Competition binding assay: Stock solutions of the compounds were prepared in DMSO and further diluted with the binding buffer to the desired concentration. Briefly, [^{3}H]-CP-55,940 (0.5 nM), non selective human CB_1 and CB_2 cannabinoid receptor was added to 6 µg of membranes from CB_1- or CB_2-overexpressing CHO cells in binding buffer (50 mM Tris-HCl, 5 mM $MgCl_2$, 2.5 mM EDTA, 0.5mg/mL BSA, pH 7.4). After 90 min at 30 °C, the incubation was stopped and the solutions were rapidly filtered over UniFilter-96 GF/C glass fiber plate, pre-soaked in PEI (0.05%) on a Filtermate UniFilter 96-Harvester (PerkinElmer) and washed 10 times with ice-cold 50 mM Tris-HCl pH 7.4. The radioactivity on the filters was measured using a TopCount NXT Microplate Scintillation Counter (PerkinElmer) using 30 µL of MicroScint 40 (PerkinElmer). Assays were performed at least in triplicate in three independent experiments. The nonspecific binding was determined in the presence of 5 µM (R)-(+)-WIN 55,212-2 (Sigma).

Cell-based HTRF cAMP assay: Cellular cAMP levels were measured using reagents supplied by Cisbio International (HTRF dynamic 2 cAMP kit). Briefly, CHO-CB_2 cells were harvested and were collected by centrifugation for 5 min at 1200 rpm. The cells were then resuspended in an appropriate final volume of culture medium and incubated with the phosphodiesterase inhibitor IBMX (0.5 mM). Cells were incubated for 15 min with the compounds at room temperature in a 384-well plate (2000 cells per well) before the addition of forskolin (3 µM) for 30 min. at room temperature. The dye d2-conjugated cAMP and Europium cryptate-conjugated anti-cAMP antibodies were added to the assay plate, according to manufacturer's instructions. After 1 hour incubation at room temperature, the plate was read on a Spectramax microplate reader (Molecular Devices) with excitation wavelength at 340 nm and emission wavelengths at 665 nm and 620 nm.

Cell culture and proliferation assay: CHO-WT, CHO-CB_2, and HT29 cells were grown at 37°C in a humidified atmosphere containing 5 % CO_2, in DMEM-GlutaMAX medium (Life technologies) supplemented with 10 % fetal bovine serum, penicillin (100 IU/mL), and streptomycin (100 µg/mL). In the cell proliferation assay, cells were plated in triplicate on 96-well plates (3.103 cells per well) and incubated for 24 h. Cells were then incubated in culture medium that contained 10 µM tested compounds. After 72 h, cell growth was estimated by the colorimetric MTS test.

X-ray Crystallography. Single-crystal X-ray diffraction analyses were performed using a Rigaku FRE+ equipped with either VHF (**11a**, **11c**) or HF Varimax confocal mirrors (**11b**,

13a) and an AFC10 goniometer and HG Saturn 724+ detector equipped with an Oxford Cryosystems low-temperature apparatus operating at T = 100(2) K.[62] CrystalClear-SM Expert 3.1 b27[63] was used to record images, process data and apply empirical absorption corrections and unit cell parameters were refined against all data. The structures were solved by charge flipping using SUPERFLIP[64] and refined on Fo^2 by full-matrix least-squares refinements using SHELXL-2012[65] as implemented within OLEX2.[66] All non-hydrogen atoms were refined with anisotropic displacement parameters and hydrogen atoms were. Hydrogen atoms were added at calculated positions except those attached to heteroatoms which were located from the difference map and restrained to a reasonable geometry. All hydrogen atoms were refined using a riding model with isotropic displacement parameters based on the equivalent isotropic displacement parameter (*Ueq*) of the parent atom. Figures were produced using OLEX2[iv]. The CIF files for the crystal structures of **11a-c** and **13a** have been deposited with the CCDC and have been given the deposition numbers 1479553-1479556 respectively.

Supporting Information. Contains scanned ^{1}H, ^{13}C NMR spectra for all compounds synthesized herein.

Acknowledgments. We are grateful to the Royal Thai Government (SS) and the China Scholarship Council (WT) for funding. We would like also to thank the reviewers for insightful comments.

Abbreviations Used:

cAMP, cyclic adenosine monophosphate;
CHO-WT, Chinese hamster ovary cells wild type;
CHO-CB_2, Chinese hamster ovary cells expressing CB2 receptors;
GPCR, G protein-coupled receptor;
HBTU, *O*-(Benzotriazol-1-yl)-*N*,*N*,*N*′,*N*′-tetramethyluronium hexafluorophosphate
SNL, spinal nerve ligation;
SI, selectivity index;
TNBS, 2,4,6-trinitrobenzenesulfonic acid;
VT, variable temperature.

References:

1. Galiègue, S.; Mary, S.; Marchand, J.; Dussossoy, D.; Carrière, D.; Carayon, P.; Bouaboula, M.; Shire, D.; Fur, G.; Casellas, P. *Eur. J. Biochem.* **1995**, *232*, 54-61.
2. Zimmer, A.; Zimmer, A. M.; Hohmann, A. G.; Herkenham, M.; Bonner, T. I. *Proc. Natl. Acad. Sci. U. S. A.* **1999**, *96*, 5780-5785.
3. Cabral, G. A.; Griffin-Thomas, L. *Expert Rev. Mol. Med.* [Online] **2009**, *11*, e3.
4. Leleu-Chavain, N.; Body-Malapel, M.; Spencer, J.; Chavatte, P.; Desreumaux, P.; Millet, R. *Curr. Med. Chem.* **2012**, *19*, 3457-3474.
5. Wright, K.; Rooney, N.; Feeney, M.; Tate, J.; Robertson, D.; Welham, M.; Ward, S. D *Gastroenterology* **2005**, *129*, 437-453.
6. Guindon, J.; Hohmann, A. G. *Br. J. Pharmacol.* **2008**, *153*, 319-334.
7. Sasso, O.; Migliore, M.; Habrant, D.; Armirotti, A.; Albani, C.; Summa, M.; Moreno-Sanz, G.; Scarpelli, R.; Piomelli, D. *FASEB J.* **2015**, *29*, 2616-2627.
8. Ashton, J. C.; Glass, M. *Curr. Neuropharmacol.* **2007**, *5*, 73-80.
9. Shoemaker, J. L.; Ruckle, M. B.; Mayeux, P. R.; Prather, P. L. *J. Pharmacol. Exp. Ther.* **2005**, *315*, 828-838.
10. Demuth, D. G.; Molleman, *Life Sci.* **2006**, *78*, 549-563.
11. Yang, W.; Li, Q.; Wang, S. Y.; Gao, F.; Qian, W. J.; Li, F.; Ji, M.; Sun, X. H.; Miao, Y.; Wang, Z. *Neuroscience* **2016**, *313*, 213-224.
12. Lunn, C.; Reich, E. P.; Fine, J.; Lavey, B.; Kozlowski, J.; Hipkin, R.; Lundell, D.; Bober, L. B. *Br. J. Pharmacol.* **2008**, *153*, 226-239.
13. Yang, P.; Myint, K. Z.; Tong, Q.; Feng, R.; Cao, H.; Almehizia, A. A.; Alqarni, M. H.; Wang, L.; Bartlow, P.; Gao, Y.; Gertsch, J.; Teramachi, J.; Kurihara, N.; Roodman, G. D.; Cheng, T.; Xie, X. Q. *J. Med. Chem.* **2012**, *55*, 9973-9987.
14. Hojnik, M.; Dobovišek, L.; Knez, Ž.; Ferk, P. *Biomed. Rep.* **2015**, *3*, 554-558.
15. Ragusa, G.; Gómez-Cañas, M.; Morales, P.; Hurst, D. P.; Deligia, F.; Pazos, R.; Pinna, G. A.; Fernández-Ruiz, J.; Goya, P.; Reggio, P. H.; Jagerovic, N.; García-Arencibia, M.; Murineddu, G. *Eur. J. Med. Chem.* **2015**, *101*, 651-667.
16. Lunn, C. A.; Fine, J. S.; Rojas-Triana, A.; Jackson, J. V.; Fan, X.; Kung, T. T.; Gonsiorek, W.; Schwarz, M. A.; Lavey, B.; Kozlowski, J. A.; Narula, S. K.; Lundell, D. J.; Hipkin, R. W.; Bober, L. A. *J. Pharmacol. Exp. Ther.* **2006**, *316*, 780-788.
17. Felder, C. C.; Joyce, K. E.; Briley, E. M.; Mansouri, J.; Mackie, K.; Blond, O.; Lai, Y.; Ma, A. L.; Mitchell, R. L. *Mol. Pharmacol.* **1995**, *48*, 443-450.
18. Ahmed, M. M.; Rajpal, S.; Sweeney, C.; Gerovac, T. A.; Allcock, B.; McChesney, S.; Patel, A. U.; Tilghman, J. I.; Miranpuri, G. S.; Resnick, D. K. *Spine J.* **2010**, *10*, 1049-1054.
19. Sreevalsan, S.; Safe, S. *Mol. Cancer Ther.* **2013**, *12*, 2483-2493.
20. Ibrahim, M. M.; Deng, H.; Zvonok, A.; Cockayne, D. A.; Kwan, J.; Mata, H. P.; Vanderah, T. W.; Lai, J.; Porreca, F.; Makriyannis, A.; Malan, T. P. Jr. *Proc. Natl. Acad. Sci. U. S. A.* **2003**, *100*, 10529-10533.
21. Storr, M. A.; Keenan, C. M.; Zhang, H.; Patel, K. D.; Makriyannis, A.; Sharkey, K. A. *Inflamm. Bowel Dis.* **2009**, *15*, 1678-1685.
22. Rinaldi-Carmona, M.; Barth, F.; Millan, J.; Derocq, J.-M.; Casellas, P.; Congy, C.; Oustric, D.; Sarran, M.; Bouaboula, M.; Calandra, B.; Portier, M.; Shire, D.; Brelière, J. C.; Le Fur, G. L. *J. Pharmacol. Exp. Ther.* **1998**, *284*, 644-650.
23. Portier, M.; Rinaldi-Carmona, M.; Pecceu, F.; Combes, T.; Poinot-Chazel, C.; Calandra, B.; Barth, F.; Le Fur, G.; Casellas, P. *J. Pharmacol. Exp. Ther.* **1999**, *288*, 582-589.
24. Rhee, M. H.; Kim, S. K. *J Vet Sci.* **2002**, *3*, 179-184.
25. Bouaboula, M.; Dussossoy, D.; Casellas, P. *J. Biol. Chem.* **1999**, *274*, 20397-20405.

26. Ross, R. A.; Brockie, H. C.; Stevenson, L. A.; Murphy, V. L.; Templeton, F.; Makriyannis, A.; Pertwee, R. G. *Br. J. Pharmacol.* **1999**, *126*, 665-672.
27. Geng, D. C.; Xu, Y. Z.; Yang, H. L.; Zhu, X. S.; Zhu, G. M.; Wang, X. B. *J. Biomed. Mater. Res., Part A* **2010**, *95*, 321-326.
28. Stern, E.; Muccioli, G. G.; Millet, R.; Goossens, J. F.; Farce, A.; Chavatte, P.; Poupaert, J. H.; Lambert, D. M.; Depreux, P.; Hénichart, J. P. *J. Med. Chem.* **2006**, *49*, 70-79.
29. Stern, E.; Muccioli, G. G.; Bosier, B.; Hamtiaux, L.; Millet, R.; Poupaert, J. H.; Hénichart, J. P.; Depreux, P.; Goossens, J. F.; Lambert, D. M. *J. Med. Chem.* **2007**, *50*, 5471-5484.
30. El Bakali, J.; Muccioli, G. G.; Renault, N.; Pradal, D.; Body-Malapel, M.; Djouina, M.; Hamtiaux, L.; Andrzejak, V.; Desreumaux, P.; Chavatte, P.; Lambert, D. M.; Millet, R. *J. Med. Chem.* **2010**, *53*, 7918-7931.
31. El Bakali, J.; Gilleron, P.; Body-Malapel, M.; Mansouri, R.; Muccioli, G. G.; Djouina, M.; Barczyk, A. l.; Klupsch, F..; Andrzejak, V.; Lipka, E.; Furman, C.; Lambert, D. M.; Chavatte, P.; Desreumaux, P.; Millet, R. *J. Med. Chem* **2012**, *55*, 8948-8952.
32. K_i values were expressed as binding affinities for CB_1/CB_2. E_{max} (GTPγS) values were expressed as the percentages of stimulation of [^{35}S]-GTPγS binding (basal value set at 100%). EC_{50} represents the concentration that exhibits the half-maximal response.
33. Ahmedi, R.; Lanez, T. *Asian J. Chem.* **2010**, *22*, 299.
34. Zanoozi, M.; Bayat, Z. Der Chemica Sinica, **2011**, *2*, 288-293.
35. Skiba, J.; Schmidt, C.; Lippmann, P.; Ensslen, P.; Wagenknecht, H. A.; Czerwieniec, R.; Brandl, F.; Ott, I.; Bernaś, T.; Krawczyk, B.; Szczukocki, D.; Kowalski, K. *Eur. J. Inorg. Chem.* [Online early access]. DOI: 10.1002/ejic.201600281. Published Obline: July 13, 2016.
36. Chavain, N.; Biot, C. *Curr. Med. Chem.* **2010**, *17*, 2729-2745.
37. Spencer, J.; Mendham, A. P.; Kotha, A. K.; Richardson, S. C.; Hillard, E. A.; Jaouen, G.; Male, L.; Hursthouse, M. B. *Dalton Trans.* **2009**, *14*, 918-921.
38. Meggers, E. *Chem. Commun.* **2009**, 1001-1010.
39. Spencer, J.; Amin, J.; Wang, M.; Packham, G.; Alwi, S. S.; Tizzard, G. J.; Coles, S. J.; Paranal, R. M.; Bradner, J. E.; Heightman, T. D. *ACS Med. Chem. Lett.* **2011**, *2*, 358-362.
40. Spencer, J.; Amin, J.; Boddiboyena, R.; Packham, G.; Cavell, B. E.; Alwi, S. S.; Paranal, R. M.; Heightman, T. D.; Wang, M.; Marsden, B.; Coxhead, P.; Guille, M.; Tizzard, G. J.; Colesf, S. J.; Bradner, J. E. *MedChemComm* **2012**, *3*, 61-64.
41. Librizzi, M.; Longo, A.; Chiarelli, R.; Amin, J.; Spencer, J.; Luparello, C. *Chem. Res. Toxicol.* **2012**, *25*, 2608-2616.
42. Patra, M.; Gasser, G.; Wenzel, M.; Merz, K.; Bandow, J. E.; Metzler-Nolte, N. *Organometallics* **2012**, *31*, 5760-5771.
43. Tauchman, J.; Süss-Fink, G.; Štěpnička, P.; Zava, O.; Dyson, P. J. *J. Organomet. Chem.* **2013**, *723*, 233-238.
44. Jaouen, G.; Vessières, A.; Top, S. *Chem. Soc. Rev.* **2015**, *44*, 8802-8817.
45. Yong, J.; Wu, X.; Liao, J.; Lu, C.; Liu, X. *Med. Chem.* **2015**, *12*, 426-431.
46. Wieczorek, A.; Błauż, A.; Zakrzewski, J.; Rychlik, B.; Plażuk, D. *ACS Med. Chem. Lett.* **2016**, *7*, 612–617.
47. Wieczorek, A.; Błauż, A.; Żal, A.; Arabshahi, H. J.; Reynisson, J.; Hartinger, C. G.; Rychlik, B.; Plażuk, D. *Chem. - Eur. J.* **2016**, 22, 11413-11421.
48. Roux, C.; Biot, C. *Future Med. Chem.* **2012**, *4*, 783-797.
49. Liu, Z. Q. *Mini-Rev. Med. Chem.* **2011**, *11*, 345-358.
50. Lewandowski, E. M.; Skiba, J.; Torelli, N. J.; Rajnisz, A.; Solecka, J.; Kowalski, K.; Chen, Y. *Chem. Commun.* **2015**, *51*, 6186-6189.

51. Saleem, M.; Yu, H.; Wang, L.; Khalid, H.; Akram, M.; Abbasi, N. M.; Huang, J. R *Anal. Chim. Acta* **2015**, *876*, 9-25.
52. Kuhn, B.; Mohr, P.; Stahl, M. *J. Med. Chem.* **2010**, *53*, 2601-2611.
53. Govaerts, S. J.; Hermans, E.; Lambert, D. M. *Eur. J. Pharm. Sci.* **2004**, *23*, 233-243.
54. Tourteau, A.; Andrzejak, V.; Body-Malapel, M.; Lemaire, L.; Lemoine, A.; Mansouri, R.; Djouina, M.; Renault, N.; EI Bakali, J.; Desreumaux, P. *Bioorg. Med. Chem.* **2013**, *21*, 5383-5394.
55. Horváth, B.; Magid, L.; Mukhopadhyay, P.; Bátkai, S.; Rajesh, M.; Park, O.; Tanchian, G.; Gao, R. Y.; Goodfellow, C. E.; Glass, M.; Mechoulam, R.; Pacher, P. *Br. J. Pharmacol.* **2012**, *165*, 2462-2478.
56. Marini, P.; Cascio, M. G.; Pertwee, R. G. *Methods Mol. Biol.* **2016**, *1412*, 85-93.
57. Marini, P.; Cascio, M. G.; King, A.; Pertwee, R. G.; Ross, R. A. *Br. J. Pharmacol.* **2013**, *169*, 887-899.
58. A $\geq$10 μM IC_{50} range is a usual "window" for bioorganometallic compounds (e.g. cisplatin, see: Bose, R. N.; Maurmann, L.; Mishur, R. J.; Yasui, L.; Gupta, S.; Grayburn, W. S.; Hofstetter, H.; Salley, T. *Proc. Natl. Acad. Sci. U. S. A.* **2009**, *105*, 18314-18319). However, in our case, our more active compounds have low nM activity, hence, a significant therapeutic window to avoid cytotoxicity at potential low doses.
59. Hagen, H.; Marzenell, P.; Jentzsch, E.; Wenz, F.; Veldwijk, M. R.; Mokhir, A. *J Med Chem.* **2012**, *55*, 924-934.
60. Hillard, E.; Vessieres, A.; Thouin, L.; Jaouen, G.; Amatore, C. *Angew. Chem. Int. Ed.* **2006**, *45*, 285-290.
61. Leonidova, A.; Anstaett, P.; Pierroz, V.; Mari, C.; Spingler, B.; Ferrari, S.; Gasser, G. *Inorg. Chem.* **2015**, *54*, 9740-9748.
62. Coles, S. J.; Gale, P. A. *Chem. Sci.* **2012**, *3*, 683-689.
63. CrystalClear, Rigaku Corporation, The Woodlands, Texas, U.S.A., (2008-2014).
64. Palatinus, L.; Chapuis, G. *J. Appl. Cryst.* **2007**, *40*, 786-790.
65. Sheldrick, G. M. *Acta Crystallogr., Sect. C: Struct. Chem.* **2015**, *71*, 3-8.
66. Dolomanov, O. V.; Bourhis, L. J.; Gildea, R. J.; Howard, J. A. K.; Puschmann, H. *J. Appl. Cryst.* **2009**, *42*, 339-341.